Probing the early Universe cosmology with NANOGrav: Possibilities and limitations

Ido Ben-Dayan, Utkarsh Kumar, Udaykrishna Thattarampilly, and Amresh Verma
Physics Department, Ariel University, Ariel 4070001, Israel

(Received 2 August 2023; accepted 11 October 2023; published 6 November 2023)

A stochastic gravitational wave background is a prediction of a number of astrophysical and cosmological phenomena including early Universe cosmology. Recently, the NANOGrav Collaboration reported conclusive evidence for a stochastic gravitational wave background. We analyze the NANOGrav signal, assuming it is of primordial origin, including the reheating phase. We use the latest measurements from NANOGrav to constrain the Universe's reheating equation of state $w_{\rm re}$, the reheating temperature $T_{\rm re}$, the tensor-to-scalar ratio r, and the tensor tilt n_t. Assuming the constant equation of state $w_{\rm re}$ to be responsible for the reheating phase, we find a preference for instant reheating, $w_{\rm re} = 0.36^{+0.15}_{-0.28}$, and a very blue tilt $n_t = 1.94^{+0.43}_{-0.88}$. We find a degeneracy between the tensor-to-scalar ratio r and $T_{\rm re}$ and suggest ways to break this degeneracy. In all cases where the reheating temperature is constrained, it is constrained to be very low, with $T_{\rm re} \leq 10^5$ GeV. We further find that a scale-invariant spectrum, as suggested by inflation, implies a stiff equation of state $w_{\rm re} = 19/3$. If extrapolated, the blue-tilted primordial spectrum that agrees with the NANOGrav signal at corresponding frequencies is incompatible with the LIGO bound. This incompatibility is another challenge for connecting NANOGrav with the primordial spectrum. We discuss a number of ways to circumvent this issue. We split the spectrum into a sum of astrophysical and primordial spectra and constrain the astrophysical and primordial components using NANOGrav data and the LIGO bound. In another attempt, we use the same data and constrain the running of the spectrum. Any of these, or a combination of such methods, can be used to reconcile the NANOGrav data and the LIGO bound with the primordial power spectrum.

DOI: 10.1103/PhysRevD.108.103507

I. INTRODUCTION

A stochastic gravitational wave background (SGWB) is a robust prediction of a number of well-motivated theories in cosmology including theories of the early Universe [1,2]. These theories generically predict a SGWB that spans a large interval of frequencies. Pulsar timing arrays (PTAs) are a well-known detection channel for nHz gravitational waves (GWs). The arrays operate by detecting the spatial correlations in the pulse arrival time for pulsars due to the perturbations in space-time induced by GWs [3]. In 2020, the NANOGrav Collaboration published an analysis of 12.5 yrs of pulsar timing data [4] reporting strong evidence for a stochastic common-spectrum process. This signal was later confirmed by a number of collaborations, including Parkes PTA (PPTA) [5] and European PTA (EPTA) [6], as well as the combined International PTA (IPTA) [7]. Recently, in 2023, various PTA experiments including NANOGrav, EPTA, PPTA, and CPTA (Chinese PTA) confirmed the presence of excess red common-spectrum signals with an amplitude of order 10^{-15} at a reference frequency range around 1 yr^{-1} [8–24]. More importantly, all recent analyses point to a GW origin of the signal. Having nearly confirmed that the measurements have a GW origin, the exciting possibility that this background signal is being sourced by fluctuations in the early Universe has been discussed in the literature [25–57].

Models of the early Universe such as inflation were introduced in order to solve problems with standard cosmology such as the horizon and flatness problem. Tensor and scalar fluctuations in the early Universe grow, stretching outside the causal horizon and reentering the horizon at a much later time. These fluctuations suggest that the origin of the structure is quantum and predict the CMB spectrum with great accuracy. Tensor perturbations produced in the early Universe are robust signatures of different early Universe paradigms and are rather insensitive to the details of the different models [58,59]. These paradigms are important contenders for the source of SGWB. The detection and characterization of the SGWB result can serve to distinguish various models and paradigms of the early Universe.

In [26], the author explores the possibility of inflationary origins of the nHz GW signal and concludes that a standard slow-roll inflationary origin is less tenable. He concludes that for the nHz GW signal to have primordial origins, the power spectrum has to be blue-tilted with a spectral index

 © 2023 American Physical Society

of $n_t = 1.8 \pm 0.3$. However, this analysis assumes instant reheating of the Universe after the inflationary phase. The effects of reheating on the GW spectrum of inflation have been discussed in literature over the years [60–62]. It has been observed that the spectral index and amplitude of the GW signal are affected by the duration of the reheating era and also by the equation of state $w_{\rm re}$ during the reheating phase [63]. In this article, we examine the possibility of a primordial origin of the nHz GW signal in the presence of a nontrivial reheating phase, while remaining agnostic about the early Universe paradigm that had been realized in nature.

We discuss the tenability of a primordial origin of the nHz signal in this renewed context. We perform a likelihood analysis of the data based on compressed likelihoods from [26]. Slow-roll inflation, where $n_t \simeq 0$, will require a stiff reheating phase of $w_{\rm re} \simeq 19/3$. A blue-tilted spectrum with $n_t \sim 1.77$ is obtained for instant reheating, in accordance with what we expect from previous works. Finally, an open reheating equation of state $w_{\rm re}$ and tensor tilt n_t result in $n_t = 1.94^{+0.43}_{-0.88}$ and $w_{\rm re} = 0.36^{+0.15}_{-0.28}$. In all cases, the reheating temperature is expected to be "low," $T_{\rm re} \leq 10^5$ GeV. Thus, within the primordial interpretation of the signal, it seems that instantaneous reheating and a primordial blue-tilted tensor spectrum are favored. This disfavors the standard canonical single-field slow-roll inflationary scenarios and favors other paradigms like a bounce [64,65], nonstandard inflation (e.g., Galileon fields, beyond slow roll, etc.) [66–76], or a GW spectrum generated by sourced fluctuations [58,59,77–86]. We briefly discuss the possibility of a bounce being the origin of the GW signal in the future directions section.

Upon assuming that the GW background we have observed is primordial, we find that the blue-tilted spectrum with a large spectral index will violate the bounds on the GW spectrum set by LIGO. A few mechanisms have been proposed in the literature such as a break in power spectrum that could explain this phenomenon. However, most of them are fine-tuned and involve a further complication of the model. We propose two purely phenomenological analyses that can alleviate this issue. One method is assuming that the spectrum can be resolved into astrophysical and primordial components and another method is assuming a significant value for the running of the spectrum. The splitting into an astrophysical part and a primordial part is very natural, and we estimate the ratio between the primordial signal and the total signal. If the astrophysical and primordial components share the same power law, then the primordial signal is at most 14.09% of the signal. Inserting the LIGO result reduces it further to a minuscule part well within the reported error bars. If we treat the astrophysical component as some fixed amplitude, we find that the primordial signal is between 34% and 55% of the PTA signal. The second method is running. The idea of running is also natural, as the constant spectral tilt is just an approximation. We find that the NANOGrav signal can be primordial and in accord with the LIGO bound with the running parameter $\alpha_t \sim -0.08$. This paper is a rough report of our analysis, and we show that it is too early to conclusively forgo the possibility of the NANOGrav signal being primordial, though such a scenario is not favored.

This article is organized as follows: In Sec. II we review the gravitational wave spectrum in the presence of a nontrivial reheating phase. In Sec. III, we discuss the spectrum of PTA signals and connect it to the primordial spectrum. Section IV deals with the details of our analysis and results. The incompatibility of the NANOGrav signal with LIGO bounds and methods of resolution for this potential problem is discussed in Sec. V. Finally, we conclude our findings and discuss future directions in Sec. VI.

II. GRAVITATIONAL WAVES IN EARLY UNIVERSE AND REHEATING

Primordial GW is one of the most exciting possible explanations for a SGWB. In this section, we briefly derive the gravitational waves spectrum generated in the early Universe. We start our discussion by considering the line element of a perturbed FLRW metric in the synchronous gauge as

$$ds^2 = a^2(\eta)\,[d\eta^2 - (\delta_{ij} + h_{ij})dx^i dx^j]. \tag{1}$$

Here, a and η are the scale factor and the conformal time, respectively, and h_{ij} is the traceless-transverse symmetric 3×3 matrix describing the GWs. The waves have two polarizations: $+, \times$, each of which is governed by the following equation in Fourier space:

$$h_k'' + 2\mathcal{H}h_k' + k^2 h_k = 0, \tag{2}$$

where $'$ denotes a derivative with respect to conformal time, $\mathcal{H}$ is the conformal Hubble parameter, and k stands for the wave number. For a given background, one can solve Eq. (2) and calculate the primordial tensor power spectrum given by

$$\mathcal{P}_T^{\rm prim} = 8\frac{k^3}{2\pi^2}|h_k|^2. \tag{3}$$

For effective model selection, we work with the following parametrization:

$$\mathcal{P}_T^{\rm prim}(k) = rA_s\left(\frac{k}{k_*}\right)^{n_t}. \tag{4}$$

Here, r and A_s are the tensor-to-scalar ratio and amplitude of the primordial scalar power spectrum evaluated at suitable pivot scale k_*, which varies from one experiment to another. We fix this pivot scale $k_* = 0.05\ \mathrm{Mpc}^{-1}$ in accordance with cosmic microwave background measurements from Planck [87]. Gravitational wave experiments such as laser interferometer (LI) and PTA measurements report their results in terms of the gravitational wave energy spectrum measured today ($\tau = \tau_0$) as

$$\Omega_{\rm GW}^{\rm prim}(f) = \frac{1}{\rho_0^{\rm crit}} \frac{d\rho_0^{\rm GW}}{d\ \ln\ f}, \tag{5}$$

where $f = \frac{9.72\times10^{-15}}{2\pi a_0} \frac{k}{\rm Mpc^{-1}}$ Hz is the present-day physical frequency of a GW associated with the comoving wave number k. The present-day GW energy spectrum $\Omega_{\rm GW}^{\rm prim}(f)$ is then related to the primordial tensor power spectrum $\mathcal{P}_T^{\rm prim}(f)$ via

$$\Omega_{\rm GW}^{\rm prim}(f) = \frac{1}{12} \left[\frac{2\pi f}{H_0}\right]^2 T_h(f) \mathcal{P}_T^{\rm prim}(f), \tag{6}$$

where $T_h(f)$ is the "tensor transfer function" derived in [63]. The tensor transfer function is expressed in the following form:

$$T_h(f) = \frac{C_2(f)C_3(f)}{2(1+z_{\rm re})^2} \left[\frac{\tilde{\gamma}^{-1/2} 2\pi f}{(1+z_{\rm re})H_0}\right]^{-4/(1+3w_{\rm re}(f))}. \tag{7}$$

Using the tensor transfer function $T_h(f)$ mentioned in Eq. (7), the present-day GW energy spectrum is written as

$$\Omega_{\rm GW}^{\rm prim}(f) = \frac{r A_s C_2(f) C_3(f) \tilde{\gamma}}{24} \left(\frac{\tilde{\gamma}^{-1/2} 2\,\pi\,f}{(1+z_{\rm re})H_0}\right)^{2\frac{3w_{\rm re}(f)-1}{3w_{\rm re}(f)+1}} \times \left(\frac{a_0 H_0 2\pi f}{k_* H_0}\right)^{n_t(f)}, \tag{8}$$

where the factors $\tilde{\gamma}$, $C_2(f)$, and $C_3(f)$ are defined as

$$\tilde{\gamma} = \frac{\Omega_{m0}}{1+z_{\rm eq}} \frac{g_*(z_{\rm re})}{g_*(z_{\rm eq})} \frac{g_{*s}^{4/3}(z_{\rm eq})}{g_{*s}^{4/3}(z_{\rm re})}, \tag{9}$$

$$C_2(f) = \frac{\Gamma^2\left(\frac{5+3w_{\rm re}(f)}{2(1+3w_{\rm re}(f))}\right)}{\pi} [1+2w_{\rm re}(f)]^{\frac{4}{1+3w_{\rm re}(f)}},$$
$$C_3(f) = \left[-\frac{10}{7} \frac{(98\Omega_{\rm fs}^3 - 589\Omega_{\rm fs}^2 + 9380\Omega_{\rm fs} - 55125)}{(15+4\Omega_{\rm fs})(50+4\Omega_{\rm fs})(105+4\Omega_{\rm fs})}\right]^2, \tag{10}$$

with Ω_{m0} denoting the relative present-day matter-energy density, $\Omega_{\rm fs} \equiv \frac{\rho^{\rm fs}}{\rho^{\rm crit}}$ as the fraction of critical density which is free-streaming relativistically (e.g., neutrinos) at redshift $z_{\rm re}$, and where $g_*(z), g_{*s}(z)$ are the number of effective relativistic degrees of freedom at the redshift z, as measured by the energy density $\rho(z)$ or the entropy density $s(z)$, respectively [63]. In the above expressions, $w_{\rm re}$ and $z_{\rm re}$ are the reheating equation of state (EOS) and the reheating redshift—i.e., the value of z at which the Universe becomes radiation dominated. Also in the expression of $\Omega_{\rm GW}$, we can replace parameter $1+z_{\rm re}$ with $T_{\rm re}$ in GeV—i.e., the temperature at the end of the reheating era—using the following relation:

$$\frac{1+z_{\rm re}}{1+z_{\rm eq}} = \frac{T_{\rm re}}{T_{\rm eq}},$$
$$1+z_{\rm re} \approx \frac{3400\times10^{11}}{80} \frac{T_{\rm re}}{\rm GeV}, \tag{11}$$

where we have used the numerical values of $z_{\rm eq}$ and $T_{\rm eq}$ from Planck 2018 data [87].

III. PULSAR TIMING ARRAYS AND CONNECTION TO THE EARLY UNIVERSE

This section reviews the SGWB spectral energy density associated with modes relevant to PTA. The present-day PTA GW spectral energy density is expressed as

$$\Omega_{\rm GW}^{\rm PTA}(f) = \frac{2\pi^2}{3H_0^2} f^2\, h_c^2(f), \tag{12}$$

where $h_c(f)$ is the power spectrum of GW at PTA scales, measured at the reference frequency, $f_{\rm yr} = 1\ {\rm yr}^{-1} \approx 3.17\times10^{-8}$ Hz. $h_c(f)$ is parametrized in the following way:

$$h_c(f) = A\left(\frac{f}{f_{\rm yr}}\right)^\beta, \tag{13}$$

where A and β are the amplitude and spectral index associated with the PTA signal. The spectral index β is related to the timing-residual cross-power spectral density index γ via $(3-\gamma)/2$. The 15-yr NANOGrav data measured the characteristic strain in the frequency range $f\in[2.0\times10^{-9}, 6\times10^{-8}]$, and these data are fitted as a power law using the following corresponding GW energy density $\Omega_{\rm GW}^{\rm PTA}$:

$$\Omega_{\rm GW}^{\rm PTA}(f) = A^2 \frac{2\pi^2}{3H_0^2} \frac{f^{5-\gamma}}{f_{\rm yr}^{\gamma-3}}. \tag{14}$$

PTA data from NANOGrav give constraints on A and γ as a joint posterior distribution. The collaboration inferred the values of $A = 6.4^{+4.2}_{-2.7}\times10^{-15}$ and $\gamma = 3.2\pm0.6$ at 2σ C.L. Let us connect these quantities to early Universe parameters. Equating Eq. (8) with Eq. (14) gives the following relation of γ with n_t and $w_{\rm re}$:

$$\gamma = 5 - n_t + 2\alpha, \tag{15}$$

where we have defined $\alpha = (\frac{1-3w_{\rm re}}{1+3w_{\rm re}})$. Similarly, the amplitude of the PTA signal is governed by the following equation:

$$A = \left(\frac{A_s C_2 C_3 H_0^2}{16\pi^2}\right)^{1/2} \tilde{\gamma}^{(1+\alpha)/2} (2\pi)^{(n_t-2\alpha)/2} \left(\frac{a_0}{k_*}\right)^{n_t/2} \times \left(\frac{T_{\rm eq}}{H_0(1+z_{\rm eq})T_{\rm re}}\right)^{-\alpha} \sqrt{r}\, {\rm yr}^{(1+\alpha-n_t/2)}. \quad (16)$$

Note that we have dropped the frequency dependence on n_t and $w_{\rm re}$ for simplicity. We will discuss the implications of frequency dependence on the reheating EOS later. The functional form of A has dependence on n_t, r, and $T_{\rm re}$. We insert the best-fit values for the cosmological parameters—i.e., $\mathcal{P}_T(k_*, \tau_i) \equiv A_s \times r = 2.1 \times 10^{-9}$ at $k_* = 0.05\ {\rm Mpc}^{-1}$, $k_{\rm eq} \approx 0.01\ {\rm Mpc}^{-1}$, $z_{\rm eq} = 3400$, $T_{\rm eq} \approx 1.25 \times 10^{29}\ {\rm Mpc}^{-1}$, $\tilde{\gamma} \approx 8.03 \times 10^{-5}$ from the Planck 2018 results [87]. It is worth mentioning that our discussion about reheating neglects transient periods from inflation to the new EOS $w_{\rm re}$, and if $w_{\rm re} \neq 1/3$, then it neglects the later transition to radiation domination. We assume that these periods were very short with practically no effect on observables. Thus, $w_{\rm re} = 1/3$ means "instantaneous reheating," while $w_{\rm re} \neq 1/3$ means a finite reheating period which ends at $T_{\rm re}$, where the Universe becomes radiation dominated. Moreover, reheating parameters impact the radiation energy density of the early Universe from GWs and result in an additional contribution. This contribution is quantified by $\Delta N_{\rm eff}$, which has effects predominantly at the scale of big bang nucleosynthesis (BBN) and recombination. The SGWB contribution to $\Delta N_{\rm eff}$ is characterized by [88–91]

$$\Delta N_{\rm eff}^{\rm GW} \approx 1.8 \times 10^5 \int_{f_{\rm min}}^{f_{\rm max}} df \frac{\Omega_{\rm GW}(f)h^2}{f}, \quad (17)$$

where the values of $f_{\rm min}$ and $f_{\rm max}$ depend on the epoch of interest and the maximum temperature reached in the big bang era. We will discuss the implications of reheating models on the integral in Eq. (17) in the next section.

IV. DATA ANALYSIS AND DISCUSSION

We use the latest NANOGrav 15-year dataset to constrain the early universe parameters. In order to extract the parameter constraints using the NANOGrav observations, we follow the analysis done in [26]. In [26], the author translated the inferred NANOGrav 15-year constraints on A and γ into constraints on inflationary parameters (r, n_t) using a grid scan. We further generalize the analysis by taking into account the effect of the era of reheating. This is realized using a constant EOS $w_{\rm re}$ and reheating temperature, $T_{\rm re}$. The data can be effectively approximated by using a Gaussian prior on $\log_{10} A$ and γ, with the following mean vector μ_{15} and covariance matrix Σ_{15} as

$$\mu_{15} \approx \left(-14.20, 3.20\right),$$

$$\Sigma_{15} \approx \begin{pmatrix} 0.127 & -0.045 \\ -0.045 & 0.021 \end{pmatrix}.$$

Using the mean vector μ_{15} and covariance matrix Σ_{15}, we define the log-likelihood function for the NANOGrav 15-year dataset as follows:

$$\ln \mathcal{L}(\theta) = -\frac{1}{2}(x(\theta) - \mu_{15})^T \Sigma_{15}^{-1} (x(\theta) - \mu_{15}). \quad (18)$$

Here, $x(\theta)$ is the vector of parameters $x(\theta) \in (\log_{10} A(\theta), \gamma(\theta))$, where θ stands for the vector of inflationary and reheating parameters. We add the NANOGrav log-likelihood given in Eq. (16) to COBAYA [92] and generate the MCMC chains with convergence criterion $R - 1 < 0.001$. We work with $\log_{10} r$ and $\log_{10} T_{\rm re}$ instead of r and $T_{\rm re}$ for statistical reasons. There exists a degeneracy between $\log_{10} r$ and $\log_{10} T_{\rm re}$, as both of them contribute to the amplitude of gravitational waves. This degeneracy can be broken in two ways. First, we can define a new parameter using the combination of $\log_{10} r$ and $\log_{10} T_{\rm re}$ as $x_{\rm re} = \log_{10}\left(r T_{\rm re}^{2\frac{1+3w_{\rm re}}{1-3w_{\rm re}}}\right)$. The second way is to fix the value of the reheating temperature ($T_{\rm re}$) / reheating EOS ($w_{\rm re}$). We explore both possibilities and illustrate our findings. Moving to the prior choices, we choose a flat prior on $\log_{10} r \in [-25, -1.44]$, $n_t \in [0, 10]$, $w_{\rm re} \in [-1/3, 1]$, and

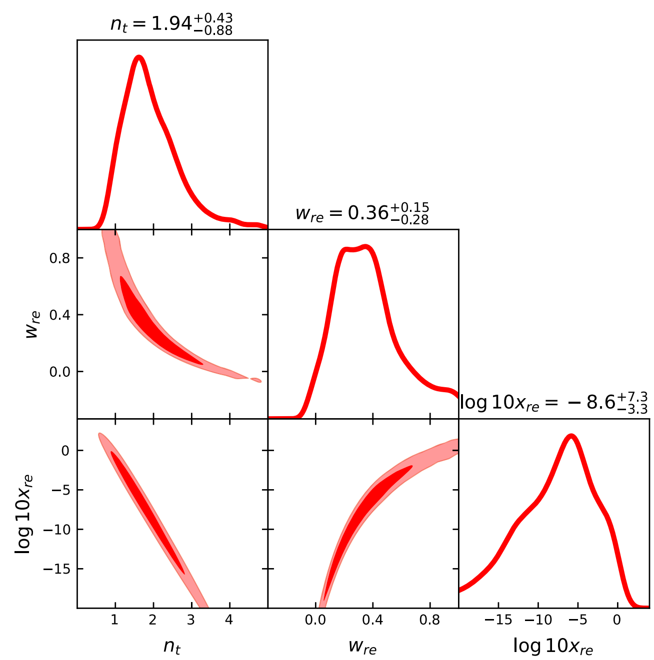

FIG. 1. Posterior distributions of primordial and reheating parameters (n_t, $w_{\rm re}$, and $x_{\rm re}$) for arbitrary reheating EOS.

TABLE I. The mean $\pm 1\sigma$ constraints on the primordial and reheating parameters inferred from the NANOGrav 15-yr data for different reheating models.

Parameter	$w_{\rm re}$ free	$w_{\rm re} = 0$	$w_{\rm re} = 1/3$	$w_{\rm re} = 1$
n_t	$1.94^{+0.43}_{-0.88}$	$3.72^{+0.23}_{-0.071}$	$1.77^{+0.18}_{-0.12}$	$0.82^{+0.16}_{-0.14}$
$\log_{10} r$	> -11.2	-19.2 ± 3.5	$-7.34^{+0.62}_{-0.85}$	> -3.36
$\log_{10}(T_{\rm re}/{\rm GeV})$	< 4.84	< -1.18	$\cdots$	< -3.06
$w_{\rm re}$	$0.36^{+0.15}_{-0.28}$	0	1/3	1
$x_{\rm re}$	$-8.6^{+7.3}_{-3.3}$	$-23.41^{+0.39}_{-1.1}$	$-7.34^{+0.62}_{-0.85}$	0.59 ± 0.72

$\log_{10} T_{\rm re}/{\rm GeV} \in [-5, 15]$. We impose the higher bound on $\log_{10} r$ such that it respects the current 95% upper limit reported from the joint analysis of Planck, WMAP, BICEP2, and BICEP3 data [93].

Figure 1 is the triangular plot showing the posterior distributions for n_t, $w_{\rm re}$, and $x_{\rm re}$ at 68% and 95% confidence levels (C.L.'s). We find $n_t = 1.94^{+0.43}_{-0.86}$ and $w_{\rm re} = 0.36^{+0.15}_{-0.28}$, a lower bound on r, and a maximal reheating temperature of $T_{\rm re} \leq 10^5$ GeV at 68% C.L.—i.e., NANOGrav data prefer instantaneous reheating and a low reheating temperature. The inferred value of n_t is linked to the best-fit power spectral density (PSD) spectral index $\gamma \approx 3.2$. The expected value of $\gamma = 13/3$ from the merging supermassive black-hole binaries (SMBHBs) corresponds to $n_T \approx 7/11$, which lies well outside the 95% C.L. Figure 1 illustrates the fact that increasing w_{re} results in a smaller inferred value of n_t.

Next, we consider the different values of $w_{\rm re} = 0$, 1/3, and 1. The 68% C.L. constraints for the above-mentioned models are tabulated in Table I. First, let us consider the canonical reheating scenario [61], which is defined by setting $w = 0$. In this scenario, we find $n_t = 3.72^{+0.23}_{-0.071}$ and $\log_{10} r = -19.2 \pm 3.5$ at 1σ credible intervals. Furthermore, the upper bound on reheating temperature comes out to be $\log_{10}(T_{\rm re}/{\rm GeV}) < -1.18$. Moving to the instantaneous reheating case—i.e., $w_{\rm re} = 1/3$—we reproduce the results presented in [26]. For the sake of completeness, we report that $n_t = 1.77^{+0.18}_{-0.12}$ and $\log_{10} r = -7.34^{+0.62}_{-0.85}$. Finally, we discuss the stiff reheating scenario ($w_{\rm re} = 1$). We report that the NANOGrav data point towards the lower tensor spectral index $n_t = 0.82^{+0.16}_{-0.14}$ and the lower bound on the tensor-to-scalar ratio, $\log_{10} r > -3.36$. The analysis of the latest 15-year NANOGrav data suggests that there is a strong correlation between the reheating EOS $w_{\rm re}$ and the inferred n_t. As a consistency check, we perform the MCMC analysis with fixed $w_{\rm re} = 19/3$, which corresponds to $n_t = 0$ from (8) and (15),[1] and as expected, we find the resulting value of $n_t = 0.165^{+0.045}_{-0.15}$ and a lower bound on $r > 0.007$ which is much closer to the upper bound given from the joint analysis of Planck, WMAP, BICEP2, and BICEP3 [93], $r < 0.036$. We show the one-dimensional normalized posterior distributions for n_t and $\log_{10} r$ for different reheating models in Fig. 2. The solid black line in Fig. 2 corresponds to the γ from SMBHBs. We have checked the robustness of our analysis for wide choices of priors of model parameters.

The 15-year NANOGrav PTA signal predicts the strong constraints on the tensor spectral index n_t and reheating EOS $w_{\rm re}$. Such a prediction of the blue spectrum and instantaneous reheating EOS set strong implications for the predictions for $\Delta N_{\rm eff}$ and the violation of upper limits on the SGWB amplitudes on interferometer scales for the primordial parameters inferred from the PTA signal. To estimate the $\Delta N_{\rm eff}$ contributions from the PTA signal, we use the integral mentioned in Eq. (17) at the BBN scales. This contribution depends on the choice of lower and upper limits appearing in Eq. (17). At BBN scales, the lower limit $f_{\rm min}$ corresponds to the size of the comoving horizon at the time of BBN, which can be safely assumed to be 10^{-10} Hz [94,95]. The choice of upper limit, $f_{\rm max}$, is quite debatable, as it depends on the reheating temperature $T_{\rm re}$. In this work, we find $f_{\rm max}$ such that the $\Delta N_{\rm eff}$ bounds from BBN are not violated from the inflationary and reheating parameters inferred from the NANOGrav data. We find the $f_{\rm max}$ corresponding to $\Delta N_{\rm eff} = 0.4$ for different reheating models discussed previously. For the arbitrary $w_{\rm re}$, using the best-fit values of model parameters, we find that the allowed value is $f_{\rm max} = 5 \times 10^{-6}$. Performing a similar exercise to other reheating models results in the allowed value of $f_{\rm max}$ spanning from $[1.4 \times 10^{-7}, 1.5 \times 10^{-5}]$. Finally, if we assume instantaneous reheating and the same tilt, the most likely value of $r \sim 10^{-7}$ and a constant n_t throughout the 62 e-folds of (i.e., $f_{\rm max} = 10^{10}$ Hz), then $n_t < 0.3$, in discord with the NANOGrav signal. We defer a more rigorous joint analysis to future work.

A much anticipated point related to the blue spectrum described by a power law is its extrapolation at least to LIGO scales. Such an extrapolation would violate upper limits from LIGO—i.e., $\Omega_{\rm GW} \leq 1.7 \times 10^{-8}$ at $f \sim 25$ Hz [96]. We find that the incorporation of the reheating phase (with constant EOS) also runs into the same problems. However, in order to avoid such a problem, there are several models in the literature that give a break in the power-law tensor power spectrum [97–102]. In the section that follows, we discuss a few ways to reconcile the GW interferometer limits (absence of GW detection by LIGO) with our results from the analysis of NANOGrav data.

V. NANOGrav IN ACCORDANCE WITH LIGO

The analysis performed in Sec. IV will violate the bounds on the GW spectrum from LIGO [96] and $\Delta N_{\rm eff}$

[1]One can derive this specific equation of state using Eq. (15) while assuming $\gamma = 3.2$. However during the analysis, we do not fix the value of $\gamma = 3.2$ in our analysis to infer n_t and r.

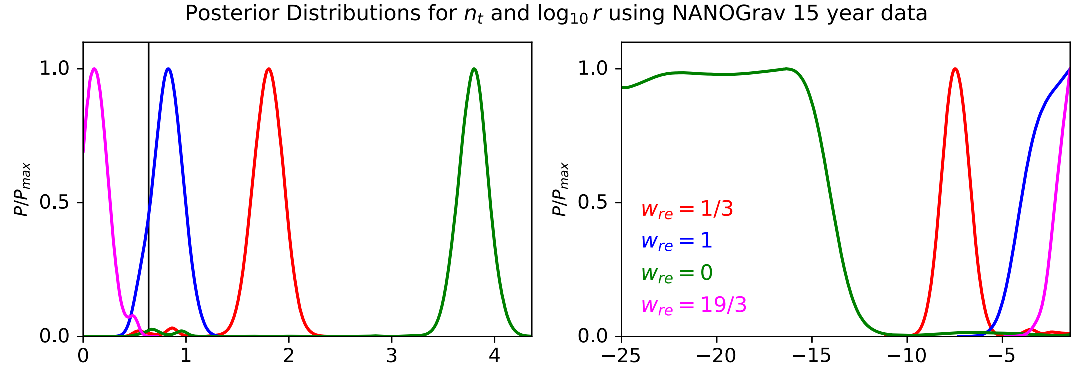

FIG. 2. The one-dimensional normalized posterior distributions for n_t (left) and $\log_{10} r$ (right) for different models of reheating. The black solid line corresponds to the spectral index of SMBHBs ($n_t = 7/11$).

if the primordial gravitational wave spectrum in Eq. (8) is extrapolated to LIGO scales. We discuss two different methods to avoid this problem in the subsections below. Note that these methods are purely phenomenological and do not require a break in the spectrum, which should be based on serious considerations.

A. Mixing of astrophysical and primordial gravitational wave backgrounds

So far, we have considered the observed SGWB from NANOGrav to be purely primordial. It could very well be that there exist several gravitational wave backgrounds (GWBs) instead of only a primordial one. An obvious way to address the bounds from LIGO and other interferometer experiments is to envisage the existence of additional astrophysical backgrounds on top of the primordial GWB. It is a challenging task to write the gravitational wave energy spectrum associated with astrophysical processes, as it depends upon several complex physical phenomena and lies beyond the scope of this paper. To account for the astrophysical GWB, we assume that the present-day astrophysical gravitational wave energy spectrum has the same frequency dependence as the primordial GWB, for simplicity. Then, the astrophysical gravitational wave energy spectrum (AGWES) today is described as

$$\Omega_{\rm GW}^{\rm Astro}(f) = A^{\rm Astro}\left(\frac{f}{f_*}\right)^{n_t+2\alpha}. \quad (19)$$

Here, $A^{\rm Astro}$ is the amplitude of the AGWES. We remind the reader that such a choice of spectrum is purely phenomenological and relevant only near the scales of PTA and becomes negligible at the interferometer scales, as these astrophysical processes such as incoherent mergers are on specific scales, unlike the primordial spectrum. After taking into account the contribution from Eq. (19), the total energy spectrum is expressed as

$$\Omega_{\rm GW}^{\rm PTA} = \Omega_{\rm GW}^{\rm Astro} + \Omega_{\rm GW}^{\rm prim}. \quad (20)$$

It is straightforward to derive the functional form of the amplitude and spectral index of PTA signal in terms of $A^{\rm Astro}$ and early Universe parameters, as was done in Sec. III. We perform the MCMC analysis with the additional parameter $A^{\rm Astro}$ along with the early Universe parameters. We work with a fixed reheating temperature, and as has been shown in Sec. IV, there exists a degeneracy between $T_{\rm re}$ and r, so fixing $T_{\rm re}$ helps us to bound r appropriately.[2]

We present the 68% C.L. constraints considering the mix of astrophysical and primordial GWBs using the NANOGrav 15-year data for different reheating models in Table II. It is worth mentioning that the inferred value of the tensor spectral index in this scenario remains pretty much unchanged. This is expected, because the relation of γ with n_t and $w_{\rm re}$ is the same as the purely primordial case. The rescaled amplitude of the AGWES, defined as $A_R^{\rm Astro} \equiv A^{\rm Astro}/(f_*)^{n_t+2\alpha}$, is constrained at 68% C.L.[3] We report $\log_{10}(A_R^{\rm Astro}) = 4.19^{+4.8}_{-0.3}$ and $\log_{10} r < -12.0$, setting $w_{\rm re}$ to be free. In this scenario,

TABLE II. The mean $\pm 1\sigma$ constraints on the model parameters inferred from the NANOGrav 15-yr data for different reheating models. Note that $A_R^{\rm Astro} \equiv \frac{A^{\rm Astro}}{(f_*)^{n_t+2\alpha}}$ is a rescaled amplitude of the astrophysical GW energy spectrum.

Parameter	$w_{\rm re}$ free	$w_{\rm re} = 0$	$w_{\rm re} = 1/3$	$w_{\rm re} = 1$
n_t	$1.62^{+0.27}_{-0.91}$	$3.76^{+0.19}_{-0.11}$	1.80 ± 0.15	0.81 ± 0.14
$\log_{10} r$	< -12.0	-29^{+11}_{-19}	< -10.7	Unconstrained
$\log_{10}(A_R^{\rm Astro})$	$4.19^{+4.6}_{-0.63}$	< 6.09	$4.15^{+4.6}_{-0.63}$	$4.43^{+4.4}_{-0.64}$
w_{re}	Unconstrained	0	1/3	1

[2]Note that fixing the value of the reheating temperature $T_{\rm re}$ does not affect the conclusions made in the analysis.

[3]We have used $f_* = f_{\rm yr}$ in the analysis.

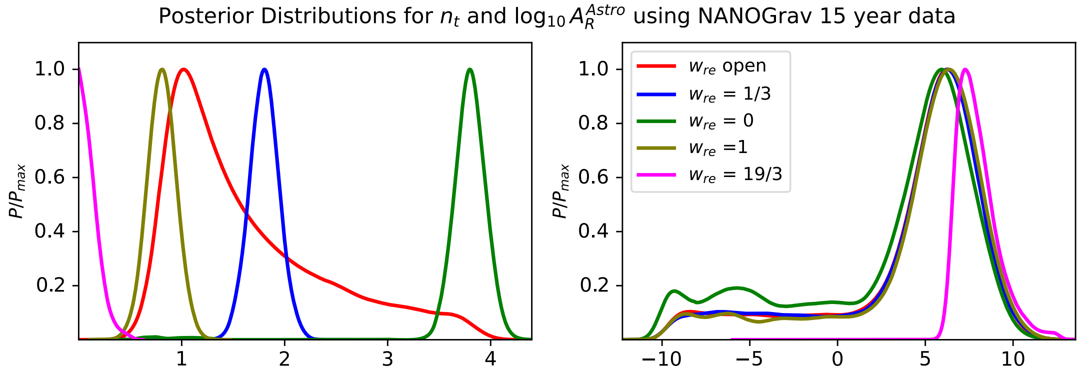

FIG. 3. The one-dimensional normalized posterior distributions for n_t and $\log_{10} A_R^{\mathrm{Astro}}$ for different models of reheating.

w_{re} is unconstrained. The results of different reheating EOSs are shown in Table II.

It is important to note that while considering the mix of astrophysical and primordial GWBs, we find upper bounds on $\log_{10} r$ to be < -12.0 and < -10.7 for the free w_{re} and instant reheating cases, respectively. For the canonical reheating scenario ($w_{\mathrm{re}} = 0$), we find $\log_{10} r = -29^{+11}_{-19}$ at 1σ limits. These inferred values of the tensor-to-scalar ratio play a significant role to satisfy the LIGO bound. One can do an independent calculation without accounting for the NANOGrav data to find the limiting value of r for given n_t. For the blue spectrum as in our case, this limiting value[4] turns out to be $\log_{10} r \approx -26$. Hence, for the extrapolated spectrum, the LIGO bound is still much stronger.

Using the inferred values of model parameters, we can estimate the amount of primordial GWB with respect to the AGWES. We define the parameter $\tilde{\beta} \equiv \Omega_{\mathrm{GW}}^{\mathrm{prim}} / \Omega_{\mathrm{GW}}^{\mathrm{Astro}}$ as the ratio of the amplitudes of the primordial GW and astrophysical GW spectrum. For the instant reheating case, using the parameter values at 68% from Table II, we find $\tilde{\beta} = 0.164$, meaning that around 14.09% of the total PTA signal could be primordial. However, imposing the LIGO constraint—i.e., $r \sim 10^{-26}$—we find that almost all of the PTA signal belongs to the astrophysical spectrum. Finally, we show the one-dimensional plots for the rescaled amplitude of the AGWES for different reheating EOSs in Fig. 3.

Next, we consider the mixing of the constant AGWES present along with the primordial GWB. That is, we consider (20), but with $\Omega_{\mathrm{GW}}^{\mathrm{Astro}} = \mathrm{constant}$. We do not perform a Bayesian analysis, as it lies beyond the scope of this article. To get a glimpse of the allowed values of model parameters, we plot (14) with 2σ credible intervals as presented in Fig. 4. We find that $n_t \in [0, 0.1]$ and $\log_{10} A^{\mathrm{Astro}} \in [-8, -7.5]$ lies within the NANOGrav band and respects the LIGO constraint as well. For the values illustrated in Fig. 4, we find that the primordial signal is between 34% and 55% of the PTA SGWB signal for $n_t = 0$, $\log_{10} A_{\mathrm{Astro}} = -7.5$ and $n_t = 0.1$, $\log_{10} A^{\mathrm{Astro}} = -8.0$.

[4]This limit on r is derived considering the results of [96].

B. Running of the spectrum

So far in the analysis, the spectrum of gravitational waves is assumed to have a constant spectral index—i.e., the spectral index is independent of the scale. The tensor spectrum of inflation typically has a running of the spectral index, albeit extremely small. The running of the spectrum for tensor perturbations α_t is defined as

$$\alpha_t = \left. \frac{d^2 \log \mathcal{P}_T^{\mathrm{prim}}}{d \log f^2} \right|_{f=f_*}. \tag{21}$$

Typically, this factor is smaller than the spectral index by a factor approximately given by the number of e-folds. Given

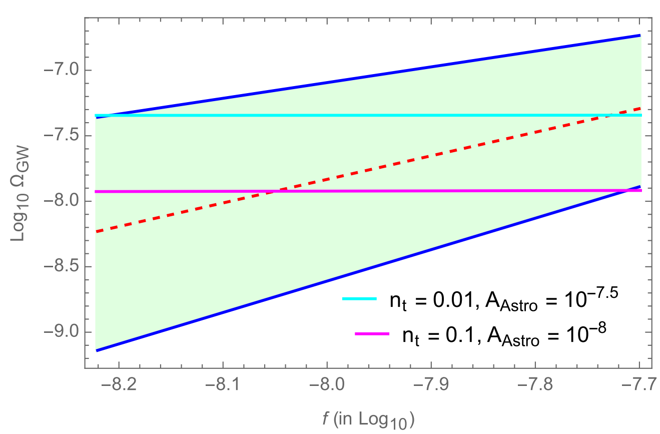

FIG. 4. Evolution of GW energy spectrum for mean $\pm 2\sigma$ values inferred from NANOGrav 15-yr results. The two blue solid lines and the one red dashed line show the gravitational wave energy spectrum for mean $+2\sigma$, mean -2σ, and mean values, respectively. The shaded green region is the allowed parameter space in accord with NANOGrav results. The cyan and magenta lines are the GW energy spectrum for parameter values respecting both NANOGrav and LIGO constraints.

TABLE III. The mean $\pm 1\sigma$ constraints on the primordial and reheating parameters with constraints on running of the spectrum obtained from LIGO bounds (last row of the table).

Parameter	$w_{\rm re}$ free	$w_{\rm re} = 0$	$w_{\rm re} = 1/3$	$w_{\rm re} = 1$
n_t	$1.94^{+0.43}_{-0.88}$	$3.72^{+0.23}_{-0.071}$	$1.77^{+0.18}_{-0.12}$	$0.82^{+0.16}_{-0.14}$
$\log_{10} r$	> -11.2	-19.2 ± 3.5	$-7.34^{+0.62}_{-0.85}$	> -3.36
$x_{\rm re}$	$-8.6^{+7.3}_{-3.3}$	$-23.41^{+0.39}_{-1.1}$	$-7.34^{+0.62}_{-0.85}$	0.59 ± 0.72
$\log_{10}(T_{\rm re}/{\rm GeV})$	< 4.78	< -1.16	$\cdots$	< -3.09
$w_{\rm re}$	$0.36^{+0.15}_{-0.28}$	0	1/3	1
α_t	-0.087 ± 0.010	$-0.0769^{+0.0051}_{-0.016}$	$-0.0847^{+0.0087}_{-0.013}$	$-0.0890^{+0.0099}_{-0.011}$

that the number of e-folds is sufficiently large, running is relatively insignificant. However, for large n_t's (that we have obtained from our analysis of NANOGrav), such as in the case of instant reheating, the running is perhaps significant enough to drive the GW amplitude small enough to a point where it is unobserved by the interferometer experiments. In order to test this hypothesis, we extrapolate the result in Eq. (8) to LIGO scales ($f \sim 25$ Hz). The amplitude of the spectrum we obtain by extrapolating Eq. (8) should satisfy the LIGO bound [96], expressed as

$$\Omega_{\rm GW}(f_{\rm LIGO}) \leq 1.7 \times 10^{-8}, \tag{22}$$

if we were to assume NANOGrav data is the primordial GW background. Assuming that running of the spectrum is significant (which is a reasonable assumption to make for large n_t), n_t in Eq. (8) is modified as

$$n_t(f) = n_t(f_{\rm yr}) + \frac{\alpha_t}{2} \log\left(\frac{f}{f_{\rm yr}}\right), \tag{23}$$

where $f_{\rm yr}$ is the frequency mode corresponding to the NANOGrav data ($f_{\rm yr} = 1\ {\rm yr}^{-1} \sim 3.17 \times 10^{-8}$ Hz). We solve Eq. (22) with parameters obtained from the likelihood analysis performed in Sec. IV. The results of our analysis are demonstrated in Table III, and the posterior distribution for the running parameter α_t in light of various reheating scenarios is presented in Fig. 5. For instantaneous reheating, if the running of the spectrum has a value $\alpha_t = -0.0847^{+0.0087}_{-0.013}$, we do not violate the bounds set by LIGO. Similarly, for our best-fit parameters, this value of running is $\alpha_t = -0.087 \pm 0.010$ for $w_{\rm re}$ free, and $-0.0769^{+0.0051}_{-0.016}$ for canonical reheating with $w_{\rm re} = 0$. Interestingly, we find that irrespective of the reheating model, $\alpha_t \sim -0.08$ can fit the NANOGrav data without violating the LIGO bounds.

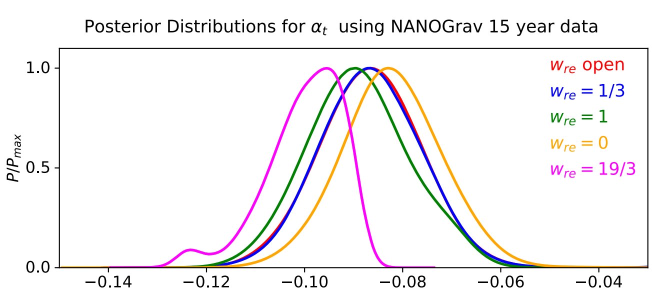

FIG. 5. The one-dimensional normalized posterior distributions for α_t for different models of reheating.

VI. CONCLUSIONS AND FUTURE DIRECTIONS

We have analyzed the NANOGrav 15-year dataset to constrain the early Universe parameters in the presence of a nontrivial reheating phase. We parametrized the power spectrum of GW as a power law. The reheating phase is characterized by an equation of state $w_{\rm re}$, and the duration of the reheating phase is determined by $T_{\rm re}$—i.e., the temperature at the end of the reheating phase. In our analysis, we find a mean value of $w_{\rm re} = 0.36 \pm 0.2$, which is very close to the equation of state of the radiation domination era, $w_{\rm rad} = 1/3$, suggesting that at the end of inflation, the Universe transitions immediately to a radiation-dominated era. While our analysis is suggestive of instantaneous reheating methods over slower reheating processes, slow reheating processes are fine as well. The sizeable error bars in $w_{\rm re}$ can accommodate alternative reheating mechanisms characterized by both stiffer ($w_{\rm re} > 1/3$) and milder ($w_{\rm re} < 1/3$) equations of state. The corresponding value of n_t is $1.94^{+0.43}_{-0.86}$ at 68% C.L., and the reheating temperature is highly limited: $T_{\rm re} \leq 10^5$ GeV.

Our analysis suggests a strong correlation between the reheating EOS and the inferred spectral index from the NANOGrav data. First, we have confirmed the results of previous studies for instant reheating. Second, we have shown that the reheating phase with stiff matter can drive down the value of the tensor spectral index of primordial gravitational waves inferred from the NANOGrav data to near-scale invariance. Finally, we infer that in general, the NANOGrav dataset tends to produce a smaller blue tilt for larger values of the reheating parameter $w_{\rm re}$. Kinetic reheating, for example, points toward a tensor spectral index of $n_t = 0.82^{+0.16}_{-0.14}$ and a lower bound on the tensor-to-scalar ratio $\log_{10} r > -3.36$, while scale invariance n_t requires a larger value of $w_{\rm re} = 19/3$. Our likelihood analysis confirmed this result for this value of $w_{\rm re}$ with

$n_t = 0.165^{+0.045}_{-0.15}$—i.e., scale invariance is 1σ away. The best-fit result for our data is a highly blue-tilted spectrum with $n_t \sim 2$ similar to bounce models. Single-field bounce scenarios are usually ruled out due to the blue-tilted scalar spectrum. However, in a series of articles pertaining to a paradigm of a sourced bounce [58,59,103,104], the authors have pointed out that this is circumvented by introducing a gauge field that sources the perturbations. In the scenario of a sourced bounce, the vacuum spectrum will remain blue-tilted. It will be interesting to examine the possibility of the NANOGrav signal being related to the vacuum spectrum of a sourced bounce.

As we pointed out earlier, the spectrum from NANOGrav is inconsistent with the upper limits from LIGO. We hypothesize that this issue can be solved in several ways. We have primarily analyzed two methods that help us resolve the inconsistency of signal with LIGO bounds. In the first case, we propose that the NANOGrav signal could be a mixture of several stochastic GW backgrounds including the primordial GW spectrum. For the sake of simplicity, we have assumed the same scale dependence for GWs from astrophysical phenomena as that of the primordial spectrum, or that the astrophysical background is a simple constant background. In the first method, the simple analysis tells us that for the LIGO bound to be respected, the portion of the GW spectrum that is primordial cannot be larger than 16%. We propose that a detailed study should be undertaken in order to distinguish astrophysical sources from primordial GWs. The constant amplitude method allows the primordial signal to be more than 34% of the total signal, and in accord with the LIGO bound, but in turn allows only a small blue tilt at the level of $n_t < 0.1$. Another proposal independent of resolving the spectrum into components has to do with a significant running of the spectrum. Our calculations show that a running of $\alpha_t \sim -0.08$ makes sure that the extrapolation of the primordial signal (with parameters obtained from NANOGrav) will respect the LIGO bounds.

We have clearly shown that the LIGO bounds can be reconciled with the NANOGrav signal being primordial. However, a significant amount of work is required in this direction. We hope that this analysis has convinced the reader that it is too early to rule out the primordial origins of this signal. During our analysis, we assumed that the reheating phase has a constant equation of state. This need not be true. Time and frequency dependence of the reheating parameters could play a role in altering the spectral index of GWs. Further analysis is required to fully understand the effect of the reheating phase on the GW spectrum at NANOGrav scales. Preferably, such analysis should combine the different datasets of PTA, CMB, and LIGO all together and include N_{eff} constraints. Assuming the primordial origins of the signal, we suggest a reheating mechanism that involves stiff matter as a way to reconcile it with the scale-invariant GW spectrum of standard canonical single-field slow-roll inflation. We save interesting questions such as resolving the spectrum and analyzing the details of the reheating phase for future works.

ACKNOWLEDGMENTS

We acknowledge the Ariel HPC Center at Ariel University for providing computing resources that have contributed to the research results reports reported within this paper.

[1] Chiara Caprini and Daniel G. Figueroa, Cosmological backgrounds of gravitational waves, Classical Quantum Gravity **35**, 163001 (2018).
[2] Arianna I. Renzini, Boris Goncharov, Alexander C. Jenkins, and Pat M. Meyers, Stochastic gravitational-wave backgrounds: Current detection efforts and future prospects, Galaxies **10**, 34 (2022).
[3] George Hobbs and Shi Dai, Gravitational wave research using Pulsar Timing Arrays, Natl. Sci. Rev. **4**, 707 (2017).
[4] Zaven Arzoumanian *et al.* (NANOGrav Collaboration), The NANOGrav 12.5 yr data set: Search for an isotropic stochastic gravitational-wave background, Astrophys. J. Lett. **905**, L34 (2020).
[5] Boris Goncharov *et al.*, On the evidence for a common-spectrum process in the search for the nanohertz gravitational-wave background with the Parkes Pulsar Timing Array, Astrophys. J. Lett. **917**, L19 (2021).
[6] S. Chen *et al.*, Common-red-signal analysis with 24-yr high-precision timing of the European Pulsar Timing Array: Inferences in the stochastic gravitational-wave background search, Mon. Not. R. Astron. Soc. **508**, 4970 (2021).
[7] J. Antoniadis *et al.*, The International Pulsar Timing Array second data release: Search for an isotropic gravitational wave background, Mon. Not. R. Astron. Soc. **510**, 4873 (2022).
[8] Gabriella Agazie *et al.* (NANOGrav Collaboration), The NANOGrav 15 yr data set: Evidence for a gravitational-wave background, Astrophys. J. Lett. **951**, L8 (2023).
[9] J. Antoniadis *et al.*, The second data release from the European Pulsar Timing Array: III. Search for gravitational wave signals, Astron. Astrophys. **678**, A50 (2023).
[10] Daniel J. Reardon *et al.*, Search for an isotropic gravitational-wave background with the Parkes Pulsar Timing Array, Astrophys. J. Lett. **951**, L6 (2023).

[11] Heng Xu *et al.*, Searching for the nano-hertz stochastic gravitational wave background with the Chinese Pulsar Timing Array Data Release I, Res. Astron. Astrophys. **23**, 075024 (2023).
[12] Gabriella Agazie *et al.* (NANOGrav Collaboration), The NANOGrav 15 yr data set: Observations and timing of 68 millisecond pulsars, Astrophys. J. Lett. **951**, L9 (2023).
[13] Gabriella Agazie, Akash Anumarlapudi, Anne M. Archibald, Paul T. Baker, Bence Bécsy, Laura Blecha, Alexander Bonilla, Adam Brazier, Paul R. Brook, Sarah Burke-Spolaor *et al.*, The nanograv 15-year data set: Constraints on supermassive black hole binaries from the gravitational wave background, Astrophys. J. Lett. **952**, L37 (2023).
[14] Gabriella Agazie *et al.* (NANOGrav Collaboration), The NANOGrav 15-year data set: Search for anisotropy in the gravitational-wave background, Astrophys. J. Lett. **956**, L3 (2023).
[15] Adeela Afzal *et al.* (NANOGrav Collaboration), The NANOGrav 15 yr data set: Search for signals from new physics, Astrophys. J. Lett. **951**, L11 (2023).
[16] Gabriella Agazie *et al.* (NANOGrav Collaboration), The NANOGrav 15 yr data set: Detector characterization and noise budget, Astrophys. J. Lett. **951**, L10 (2023).
[17] Aaron D. Johnson, Patrick M. Meyers, Paul T. Baker, Neil J. Cornish, Jeffrey S. Hazboun, Tyson B. Littenberg, Joseph D. Romano, Stephen R. Taylor, Michele Vallisneri, Sarah J. Vigeland *et al.*, The NANOGrav 15-year gravitational-wave background analysis pipeline, arXiv:2306.16223.
[18] Gabriella Agazie *et al.* (NANOGrav Collaboration), The NANOGrav 15 yr data set: Bayesian limits on gravitational waves from individual supermassive black hole binaries, Astrophys. J. Lett. **951**, L50 (2023).
[19] J. Antoniadis *et al.*, The second data release from the European Pulsar Timing Array: II. Customised pulsar noise models for spatially correlated gravitational waves, Astron. Astrophys. **678**, A49 (2023).
[20] J. Antoniadis *et al.*, The second data release from the European Pulsar Timing Array: IV. Search for continuous gravitational wave signals, arXiv:2306.16226.
[21] J. Antoniadis *et al.*, The second data release from the European Pulsar Timing Array: V. Implications for massive black holes, dark matter and the early Universe, arXiv:2306.16227.
[22] Clemente Smarra *et al.* (European Pulsar Timing Array Collaboration), The second data release from the European Pulsar Timing Array: VI. Challenging the ultralight dark matter paradigm, arXiv:2306.16228.
[23] Daniel J. Reardon *et al.*, The gravitational-wave background null hypothesis: Characterizing noise in millisecond pulsar arrival times with the Parkes Pulsar Timing Array, Astrophys. J. Lett. **951**, L7 (2023).
[24] Andrew Zic *et al.*, The Parkes Pulsar Timing Array third data release, arXiv:2306.16230.
[25] Sunny Vagnozzi, Implications of the NANOGrav results for inflation, Mon. Not. R. Astron. Soc. **502**, L11 (2020).
[26] Sunny Vagnozzi, Inflationary interpretation of the stochastic gravitational wave background signal detected by Pulsar Timing Array experiments, J. High Energy Astrophys. 39 (**2023**) 81.
[27] Satyabrata Datta, Inflationary gravitational waves, pulsar timing data and low-scale-leptogenesis, arXiv:2307.00646.
[28] George Lazarides, Rinku Maji, and Qaisar Shafi, Superheavy quasi-stable strings and walls bounded by strings in the light of NANOGrav 15 year data, arXiv:2306.17788.
[29] Zhi-Chao Zhao, Qing-Hua Zhu, Sai Wang, and Xin Zhang, Exploring the equation of state of the early universe: Insights from BBN, CMB, and PTA observations, arXiv:2307.13574.
[30] Barnali Das, Nur Jaman, and M. Sami, Gravitational waves background (NANOGrav) from quintessential inflation, arXiv:2307.12913.
[31] Mohammad Ali Gorji, Misao Sasaki, and Teruaki Suyama, Extra-tensor-induced origin for the PTA signal: No primordial black hole production, Phys. Lett. B **846**, 138214 (2023).
[32] Moslem Ahmadvand, Ligong Bian, and Soroush Shakeri, A heavy QCD axion model in light of Pulsar Timing Arrays, arXiv:2307.12385.
[33] Zhao Zhang, Chengfeng Cai, Yu-Hang Su, Shiyu Wang, Zhao-Huan Yu, and Hong-Hao Zhang, Nano-Hertz gravitational waves from collapsing domain walls associated with freeze-in dark matter in light of pulsar timing array observations, arXiv:2307.11495.
[34] M. Bousder, A. Riadsolh, A. El Fatimy, M. El Belkacemi, and H. Ez-Zahraouy, Implications of the NANOGrav results for primordial black holes and Hubble tension, arXiv:2307.10940.
[35] Lorenzo Valbusa Dall'Armi, Alina Mierna, Sabino Matarrese, and Angelo Ricciardone, Adiabatic or non-adiabatic? Unraveling the nature of initial conditions in the cosmological gravitational wave background, arXiv:2307.11043.
[36] Yanou Cui, Soubhik Kumar, Raman Sundrum, and Yuhsin Tsai, Unraveling cosmological anisotropies within stochastic gravitational wave backgrounds, arXiv:2307.10360.
[37] Spyros Basilakos, Dimitri V. Nanopoulos, Theodoros Papanikolaou, Emmanuel N. Saridakis, and Charalampos Tzerefos, Gravitational wave signatures of no-scale supergravity in NANOGrav and beyond, arXiv:2307.08601.
[38] Shyam Balaji, Guillem Domènech, and Gabriele Franciolini, Scalar-induced gravitational wave interpretation of PTA data: The role of scalar fluctuation propagation speed, arXiv:2307.08552.
[39] Graciela B. Gelmini and Jonah Hyman, Catastrogenesis with unstable ALPs as the origin of the NANOGrav 15 yr gravitational wave signal, arXiv:2307.07665.
[40] Masaki Yamada and Kazuya Yonekura, Dark baryon from pure Yang-Mills theory and its GW signature from cosmic strings, J. High Energy Phys. 09 (2023) 197.
[41] E. Babichev, D. Gorbunov, S. Ramazanov, R. Samanta, and A. Vikman, NANOGrav spectral index $\gamma = 3$ from melting domain walls, arXiv:2307.04582.
[42] Wilfried Buchmuller, Valerie Domcke, and Kai Schmitz, Metastable cosmic strings, arXiv:2307.04691.
[43] Zhi-Qiang You, Zhu Yi, and You Wu, Constraints on primordial curvature power spectrum with pulsar timing arrays, arXiv:2307.04419.

[44] Alberto Salvio, Supercooling in radiative symmetry breaking: Theory extensions, gravitational wave detection and primordial black holes, arXiv:2307.04694.

[45] Yann Gouttenoire, First-order phase transition interpretation of PTA signal produces solar-mass black holes, arXiv:2307.04239.

[46] Michael Geller, Subhajit Ghosh, Sida Lu, and Yuhsin Tsai, Challenges in Interpreting the NANOGrav 15-year data set as early universe gravitational waves produced by ALP induced instability, arXiv:2307.03724.

[47] Xiao Kang Du, Ming Xia Huang, Fei Wang, and Ying Kai Zhang, Did the nHZ gravitational waves signatures observed by NANOGrav indicate multiple sector SUSY breaking? arXiv:2307.02938.

[48] Géraldine Servant and Peera Simakachorn, Constraining post-inflationary axions with Pulsar Timing Arrays, arXiv:2307.03121.

[49] Yu-Mei Wu, Zu-Cheng Chen, and Qing-Guo Huang, Cosmological interpretation for the stochastic signal in Pulsar Timing Arrays, arXiv:2307.03141.

[50] Xiu-Fei Li, Probing the high temperature symmetry breaking with gravitational waves from domain walls, arXiv:2307.03163.

[51] Lang Liu, Zu-Cheng Chen, and Qing-Guo Huang, Probing the equation of state of the early Universe with Pulsar Timing Arrays, arXiv:2307.14911.

[52] Lang Liu, Zu-Cheng Chen, and Qing-Guo Huang, Implications for the non-Gaussianity of curvature perturbation from Pulsar Timing Arrays, arXiv:2307.01102.

[53] V. K. Oikonomou, Flat energy spectrum of primordial gravitational waves versus peaks and the NANOGrav 2023 observation, Phys. Rev. D **108**, 043516 (2023).

[54] Daniel G. Figueroa, Mauro Pieroni, Angelo Ricciardone, and Peera Simakachorn, Cosmological background interpretation of Pulsar Timing Array Data, arXiv:2307.02399.

[55] Caner Unal, Alexandros Papageorgiou, and Ippei Obata, Axion-gauge dynamics during inflation as the origin of Pulsar Timing Array signals and primordial black holes, arXiv:2307.02322.

[56] Xuce Niu and Moinul Hossain Rahat, NANOGrav signal from axion inflation, arXiv:2307.01192.

[57] Yi-Fu Cai, Xin-Chen He, Xiaohan Ma, Sheng-Feng Yan, and Guan-Wen Yuan, Limits on scalar-induced gravitational waves from the stochastic background by pulsar timing array observations, arXiv:2306.17822.

[58] Ido Ben-Dayan, Gravitational waves in bouncing cosmologies from gauge field production, J. Cosmol. Astropart. Phys. 09 (2016) 017.

[59] Ido Ben-Dayan and Judy Kupferman, Sourced scalar fluctuations in bouncing cosmology, J. Cosmol. Astropart. Phys. 07 (2019) 050; 12 (2020) E01.

[60] Jerome Martin, Christophe Ringeval, and Vincent Vennin, Observing inflationary reheating, Phys. Rev. Lett. **114**, 081303 (2015).

[61] Liang Dai, Marc Kamionkowski, and Junpu Wang, Reheating constraints to inflationary models, Phys. Rev. Lett. **113**, 041302 (2014).

[62] Kaloian D. Lozanov, Lectures on reheating after inflation, arXiv:1907.04402.

[63] Latham A. Boyle and Alessandra Buonanno, Relating gravitational wave constraints from primordial nucleosynthesis, pulsar timing, laser interferometers, and the CMB: Implications for the early Universe, Phys. Rev. D **78**, 043531 (2008).

[64] D. Battefeld and Patrick Peter, A critical review of classical bouncing cosmologies, Phys. Rep. **571**, 1 (2015).

[65] Justin Khoury, Burt A. Ovrut, Paul J. Steinhardt, and Neil Turok, The Ekpyrotic universe: Colliding branes and the origin of the hot big bang, Phys. Rev. D **64**, 123522 (2001).

[66] Tsutomu Kobayashi, Masahide Yamaguchi, and Jun'ichi Yokoyama, G-inflation: Inflation driven by the Galileon field, Phys. Rev. Lett. **105**, 231302 (2010).

[67] Hiroaki W. H. Tahara and Tsutomu Kobayashi, Nanohertz gravitational waves from a null-energy-condition violation in the early universe, Phys. Rev. D **102**, 123533 (2020).

[68] Yun-Song Piao and Yuan-Zhong Zhang, Phantom inflation and primordial perturbation spectrum, Phys. Rev. D **70**, 063513 (2004).

[69] Andrei Gruzinov, Elastic inflation, Phys. Rev. D **70**, 063518 (2004).

[70] Masaki Satoh and Jiro Soda, Higher curvature corrections to primordial fluctuations in slow-roll inflation, J. Cosmol. Astropart. Phys. 09 (2008) 019.

[71] Yosuke Mishima and Tsutomu Kobayashi, Revisiting slow-roll dynamics and the tensor tilt in general single-field inflation, Phys. Rev. D **101**, 043536 (2020).

[72] Yi-Fu Cai, Jinn-Ouk Gong, Shi Pi, Emmanuel N. Saridakis, and Shang-Yu Wu, On the possibility of blue tensor spectrum within single field inflation, Nucl. Phys. **B900**, 517 (2015).

[73] Jinn-Ouk Gong, Blue running of the primordial tensor spectrum, J. Cosmol. Astropart. Phys. 07 (2014) 022.

[74] Xingang Chen, Hassan Firouzjahi, Mohammad Hossein Namjoo, and Misao Sasaki, A single field inflation model with large local non-Gaussianity, Europhys. Lett. **102**, 59001 (2013).

[75] Chunshan Lin, Massive graviton on a spatial condensate, Phys. Lett. B **738**, 386 (2014).

[76] A. Emir Gumrukcuoglu, Sachiko Kuroyanagi, Chunshan Lin, Shinji Mukohyama, and Norihiro Tanahashi, Gravitational wave signal from massive gravity, Classical Quantum Gravity **29**, 235026 (2012).

[77] Neil Barnaby, Enrico Pajer, and Marco Peloso, Gauge field production in axion inflation: Consequences for monodromy, non-Gaussianity in the CMB, and gravitational waves at interferometers, Phys. Rev. D **85**, 023525 (2012).

[78] Yi Wang and Wei Xue, Inflation and alternatives with blue tensor spectra, J. Cosmol. Astropart. Phys. 10 (2014) 075.

[79] Chiara Caprini and Lorenzo Sorbo, Adding helicity to inflationary magnetogenesis, J. Cosmol. Astropart. Phys. 10 (2014) 056.

[80] Shinji Mukohyama, Ryo Namba, Marco Peloso, and Gary Shiu, Blue tensor spectrum from particle production during inflation, J. Cosmol. Astropart. Phys. 08 (2014) 036.

[81] Mar Bastero-Gil, Arjun Berera, Rudnei O. Ramos, and João G. Rosa, Observational implications of matter-genesis during inflation, J. Cosmol. Astropart. Phys. 10 (2014) 053.

[82] Jessica L. Cook and Lorenzo Sorbo, Particle production during inflation and gravitational waves detectable by ground-based interferometers, Phys. Rev. D **85**, 023534 (2012); **86**, 069901(E) (2012).

[83] Daniel Carney, Willy Fischler, Ely D. Kovetz, Dustin Lorshbough, and Sonia Paban, Rapid field excursions and the inflationary tensor spectrum, J. High Energy Phys. 11 (2012) 042.

[84] Leonardo Senatore, Eva Silverstein, and Matias Zaldarriaga, New sources of gravitational waves during inflation, J. Cosmol. Astropart. Phys. 08 (2014) 016.

[85] Sabino Matarrese, Silvia Mollerach, and Marco Bruni, Second order perturbations of the Einstein–de Sitter universe, Phys. Rev. D **58**, 043504 (1998).

[86] Matteo Biagetti, Matteo Fasiello, and Antonio Riotto, Enhancing inflationary tensor modes through spectator fields, Phys. Rev. D **88**, 103518 (2013).

[87] N. Aghanim *et al.* (Planck Collaboration), Planck 2018 results: VI. Cosmological parameters, Astron. Astrophys. **641**, A6 (2020); **652**, C4(E) (2021).

[88] Sachiko Kuroyanagi, Tomo Takahashi, and Shuichiro Yokoyama, Blue-tilted tensor spectrum and thermal history of the universe, J. Cosmol. Astropart. Phys. 02 (2015) 003.

[89] Ido Ben-Dayan, Brian Keating, David Leon, and Ira Wolfson, Constraints on scalar and tensor spectra from N_{eff}, J. Cosmol. Astropart. Phys. 06 (2019) 007.

[90] Sunny Vagnozzi and Abraham Loeb, The challenge of ruling out inflation via the primordial graviton background, Astrophys. J. Lett. **939**, L22 (2022).

[91] William Giarè, Matteo Forconi, Eleonora Di Valentino, and Alessandro Melchiorri, Towards a reliable calculation of relic radiation from primordial gravitational waves, Mon. Not. R. Astron. Soc. **520**, 2 (2023).

[92] Jesus Torrado and Antony Lewis, COBAYA: Code for Bayesian analysis of hierarchical physical models, J. Cosmol. Astropart. Phys. 05 (2021) 057.

[93] P. A. R. Ade *et al.* (BICEP, Keck Collaborations), Improved constraints on primordial gravitational waves using Planck, WMAP, and BICEP/Keck observations through the 2018 observing season, Phys. Rev. Lett. **127**, 151301 (2021).

[94] Tristan L. Smith, Elena Pierpaoli, and Marc Kamionkowski, A new cosmic microwave background constraint to primordial gravitational waves, Phys. Rev. Lett. **97**, 021301 (2006).

[95] Giovanni Cabass, Luca Pagano, Laura Salvati, Martina Gerbino, Elena Giusarma, and Alessandro Melchiorri, Updated constraints and forecasts on primordial tensor modes, Phys. Rev. D **93**, 063508 (2016).

[96] R. Abbott *et al.* (KAGRA, Virgo, and LIGO Scientific Collaborations), Upper limits on the isotropic gravitational-wave background from Advanced LIGO and Advanced Virgo's third observing run, Phys. Rev. D **104**, 022004 (2021).

[97] Bruce Allen and Ram Brustein, Detecting relic gravitational radiation from string cosmology with LIGO, Phys. Rev. D **55**, 3260 (1997).

[98] Sai Wang, Zhi-Chao Zhao, Jun-Peng Li, and Qing-Hua Zhu, Exploring the implications of 2023 Pulsar Timing Array datasets for scalar-induced gravitational waves and primordial black holes, arXiv:2307.00572.

[99] Micol Benetti, Leila Lobato Graef, and Sunny Vagnozzi, Primordial gravitational waves from NANOGrav: A broken power-law approach, Phys. Rev. D **105**, 043520 (2022).

[100] Seyed Ali Hosseini Mansoori, Fereshteh Felegray, Alireza Talebian, and Mohammad Sami, PBHs and GWs from $\mathbb{T}^2$-inflation and NANOGrav 15-year data, J. Cosmol. Astropart. Phys. 08 (2023) 067.

[101] Kingman Cheung, C. J. Ouseph, and Po-Yan Tseng, NANOGrav signal and PBH from the modified Higgs inflation, arXiv:2307.08046.

[102] Sayantan Choudhury, Single field inflation in the light of NANOGrav 15-year Data: Quintessential interpretation of blue tilted tensor spectrum through non-bunch Davies initial condition, arXiv:2307.03249.

[103] Michał Artymowski, Ido Ben-Dayan, and Udaykrishna Thattarampilly, Sourced fluctuations in generic slow contraction, J. Cosmol. Astropart. Phys. 06 (2021) 010.

[104] Ido Ben-Dayan and Udaykrishna Thattarampilly, Requiem to "Proof of Inflation" or sourced fluctuations in a non-singular bounce, arXiv:2308.00256.